# CONTINUUM THEORY OF DISLOCATIONS VERSUS FINITE ELEMENT METHOD

Horacio Antunez and Paweł Dłużewski

*Institute of Fundamental Technological Research – Polish Academy of Sciences*
*Świętokrzyska 21, 00-049 Warsaw - POLAND*

## Resumen

Se presenta la simulación computacional de deformaciones elasto-plásticas inducidas por movimiento de defectos en cristales. Se adopta un modelo constitutivo que vincula las fuerzas impulsoras con la velocidad de las dislocaciones. El modelo hace uso de las relaciones entre el tensor de deformaciones plásticas y el de densidad de dislocaciones. Dado un cristal bajo ciertas condiciones iniciales y de contorno, se obtiene la evolucion del campo de dislocaciones y de las deformaciones elasto-plásticas mediante la resolución acoplada del sistema de ecuaciones resultante de la ecuacion de equilibrio y del balance de dislocaciones para cada paso de tiempo. Se discretiza el sistema de ecuaciones mediante el método de los elementos finitos. Se ilustra el modelo a través de la simulación del movimiento de un campo de dislocaciones de borde que produce una banda de deformaciones de corte en un monocristal.

## Abstract

The computer simulation of elastic–plastic deformations induced by crystal defect motion is presented. The constitutive model relates the driving forces with dislocation velocities. The model makes use of the coupling between the plastic deformation rate and the dislocation velocity. Given a crystal under certain boundary and initial conditions the evolution of both dislocation field and elastic-plastic deformations is obtained by solving the coupled system of equations resulting from the equilibrium equation and the dislocation balance for each time step. The set of equations is discretized by the finite element method. As an example the movement of edge dislocation field inducing shear band deformation in a monocrystal is considered.

## Introduction

In continuum mechanics two different approaches may be identified for dislocation modelling. The first one considers the dislocations as discrete lines in an elastic continuum; the second, as a 3-dimensional region the dimensions of which are determined by the assumed size of the dislocation core. An important drawback of the first approach is the discrete character of the dislocation, which represents a singularity within the continuum description of crystal deformation. As a result stresses grow to infinity along the dislocation line. The second drawback, even more serious, is that as a discrete model it cannot be implemented in continuum mechanics based on numerical methods, e.g. the finite element method. In spite of this, many attempts are presently undertaken for dislocation modelling in a finite element context. Among them, Stigh [6] makes use of a cut-off and welding technique to insert the elements which simulates the dislocation. However, such an approach

in practice does not allow to model the dislocation movement. In other approach Canova *et al.* [1] have used a model where discrete dislocations travel across the elements "jumping" from node to node. In this approach the direction of dislocation movement is limited by the discretization.

In the present work the method developed by Dluzewski and Antunez [3] has been used.

### Linear continuum dislocation theory

In the framework of the linear continuum theory of dislocations, the gradient of displacements can be decomposed as follows

$$\nabla u = \varpi + \varepsilon_e + \varepsilon_p \tag{1}$$

where $\varpi$ is the antisymmetric tensor of crystal lattice rotation, $\varepsilon_e$ is the elastic deformation tensor while $\varepsilon_p$ is the (generally non-symmetric) plastic deformation tensor.

The dislocation density tensor is defined as

$$\alpha_d \overset{df}{=} \operatorname{curl} \varepsilon_p \tag{2}$$

(see e.g. [4]), which reads, in index notation

$$\alpha_{dij} = \varepsilon_{pim,n} e_{jmn} \tag{3}$$

where $e_{jmn}$ is the permutation tensor. In the linear theory it is also assumed that the plastic deformation rate satisfies the kinematic condition

$$\dot{\varepsilon}_p = \alpha_d \times v_d \tag{4}$$

where $v_d$ is the vector of the local velocity of discolations. The absolute dislocation velocity is written as $v + v_d$ where $v$ is the velocity of material (mass velocity).

### Set of equations and unknowns

The dislocation field motion for quasi-static isothermal elastic–plastic problems can be described by the following set

$$\operatorname{div}\sigma = 0 \tag{5}$$

$$\alpha_p = \operatorname{curl}\varepsilon_p \tag{6}$$

$$\dot{\varepsilon}_p = \alpha_p \times v_p \tag{7}$$

with the constitutive equation relating the stress and the dislocation velocity $v_d$

$$\sigma = D(\nabla u - \varepsilon_p) \tag{8}$$

$$v_d = \frac{1}{\rho_d}\lambda_d f_d \tag{9}$$

where $D$ and $\lambda$ are respectively fourth and second order tensors depending on the material constants, while $f_d$ is the Peach-Koehler force [5] defined for a continuous dislocation density field. This force is expressed by

$$f_{di} = \sigma_{jk}\alpha_{djl}e_{ikl} \tag{10}$$

In order to reduce the number of unknowns we have additionally restricted the problem to the conservative motion of edge dislocations. Moreover, limiting the dislocation motion to pure slip, the plastic deformation tensor reads

$$\varepsilon_p = \gamma_p \varepsilon_0 \tag{11}$$

where the tensor $\varepsilon_0$ is taken as a constant and is expressed by

$$\varepsilon_0 = \frac{b_d}{|b_d|} \otimes (1 \times \frac{b_d}{|b_d|}) \tag{12}$$

where $\mathbf{b_d}$ and $\mathbf{l}$ are the Burgers vector and the unit direction vector along the dislocation line, respectively. Taking into account the preceding relations, the equation system (5)-(7) reduces to the following set

$$\mathrm{div}\boldsymbol{\sigma} = \mathbf{0} \tag{13}$$

$$\dot{\rho}_d = -\mathrm{div}(\rho_d \mathbf{v_d}) \tag{14}$$

$$\dot{\gamma}_p = v_d \rho_d b_d \tag{15}$$

where $b_d = |\mathbf{b_d}|$, $v_d = |\mathbf{v_d}|$, while the stresses and dislocation velocity fulfill the following constitutive equations

$$\boldsymbol{\sigma} = \mathbf{D}(\nabla \mathbf{u} - \gamma_p \boldsymbol{\varepsilon}_o) \tag{16}$$

$$v_d = \lambda_d b_d \boldsymbol{\sigma} : \boldsymbol{\varepsilon}_o \tag{17}$$

$\lambda_d$ is the nonzero component of $\boldsymbol{\lambda}_d$ such that

$$\boldsymbol{\lambda}_d = \lambda_d \frac{\mathbf{b_d}}{|\mathbf{b_d}|} \otimes (\mathbf{l} \times \frac{\mathbf{b_d}}{|\mathbf{b_d}|}) \tag{18}$$

Summarizing, the unknowns are: displacements – $u_x$, $u_y$, scalar dislocation density – $\rho_d$, and plastic deformation $\gamma_p$.

### Numerical algorithm

The numerical simulation of dislocation motion was carried out by introducing the corresponding numerical procedures developed to this purpose to the FEAP program [7]. Available elastic–plastic programmes (like the one quoted) calculate each deformation increment without distinction of elastic and plastic component. These models are approximated and do not assure good results during unloading. Therefore in the presented algorithm we have chosen a more exact, but difficult approach based on the separate modelling of elastic and plastic deformations.

The equation set to be solved is given by equations (13)-(15). They constitute a nonlinear coupled set in which the displacements $u_x, u_y$, dislocation density $\rho_d$ and plastic deformation $\gamma_p$ are the unknowns. The latter is treated as internal variable and is calculated by integration along the process history, while the other three are nodal variables. Time integration is performed by the (implicit) backward Euler algorithm. The balance equation for forces is written in rate form. After discretization the algebraic equation system reads

$$\begin{bmatrix} \mathbf{C_u} & \mathbf{0} \\ \mathbf{0} & \mathbf{C_\rho} \end{bmatrix} \begin{bmatrix} \dot{\mathbf{a}}_u \\ \dot{\mathbf{a}}_\rho \end{bmatrix} + \begin{bmatrix} \mathbf{P_u} \\ \mathbf{P_\rho} \end{bmatrix} = \begin{bmatrix} \dot{\mathbf{f}}_u \\ \mathbf{f}_\rho \end{bmatrix} \tag{19}$$

where $\mathbf{a}_u$, $\mathbf{a}_\rho$, $\mathbf{f}_u$ and $\mathbf{f}_\rho$ are the displacement, dislocation density, nodal forces and nodal dislocation flow vectors, respectively, while $\mathbf{a}_\gamma$ is the plastic deformation vector at the Gauss integration points. Moreover,

$$\mathbf{C_u} = \int_v \nabla^T \mathbf{W_u} \mathbf{D} \nabla \mathbf{N} dv \tag{20}$$

$$\mathbf{C_\rho} = \int_v \mathbf{W_\rho} \otimes \mathbf{N} dv \tag{21}$$

$$\mathbf{P_u} = -\int_v \nabla^T \mathbf{W_u} \mathbf{D} \boldsymbol{\varepsilon}_o b_d \rho_d v_d dv \tag{22}$$

$$\mathbf{P_\rho} = \int_v \nabla^T \mathbf{W_\rho} \frac{\mathbf{b_d}}{|\mathbf{b_d}|} v_d \rho_d dv \tag{23}$$

where $\mathbf{W_u}$ and $\mathbf{W_\rho}$ are weight functions for displacements and dislocation density, respectively. $\mathbf{N}$ is the shape function and $\rho_{d_i}$ and $v_{d_i}$ are, respectively, the dislocation density and velocity. This velocity is determined at the Gauss points as

$$v_d = \lambda_d b_d \mathbf{D} \boldsymbol{\varepsilon}_o (\nabla \mathbf{N} \otimes \mathbf{a}_u - \gamma_p \boldsymbol{\varepsilon}_o) \tag{24}$$
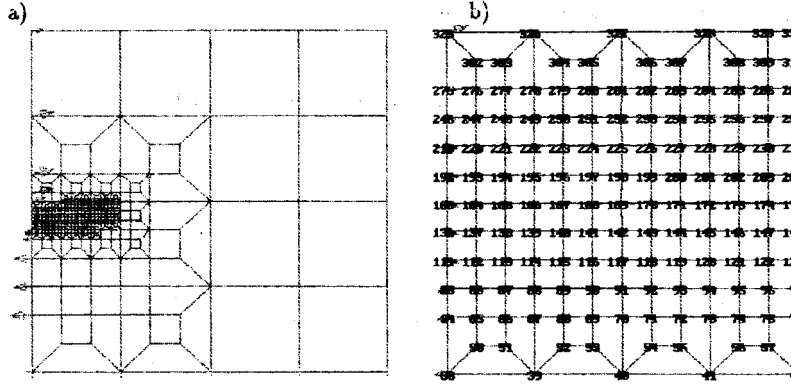
Figure 1: a) Element grid with loading and boundary conditions, b) detail of the mesh refined region

The matrix equation (19) can be considered as the nonlinear ordinary differential equation system with respect to the a vector

$$\mathbf{C}\dot{\mathbf{a}} + \mathbf{P}(\mathbf{a}) = \mathbf{f} \tag{25}$$

By use of the backward Euler scheme for time integration, equation (25) has been replaced by the relation

$$\frac{1}{\Delta t}\mathbf{C}\ (\mathbf{a}_{n+1} - \mathbf{a}_n) + \mathbf{P}(\mathbf{a}_{n+1}) = \mathbf{f} \tag{26}$$

from which we obtain $\mathbf{a}_{n+1}$ for $t_{n+1}$. In that case, (26) can be solved by the Newton–Raphson method. Then the tangent stiffness matrix has the form

$$\mathbf{K}_T^{(i)} = \frac{\mathbf{C}}{\Delta t} + \frac{\partial \mathbf{P}}{\partial \mathbf{a}_{n+1}^{(i)}} \tag{27}$$

After substituting (22) and (23) and carrying out the differentiation we get

$$\frac{\partial \mathbf{P}}{\partial \mathbf{a}_{n+1}^{(i)}} \approx \left[ \begin{array}{cc} \int_v \nabla^T \mathbf{W}_u \mathbf{D}\varepsilon_o b_d \rho_d \lambda_d b_d \varepsilon_o \mathbf{D}\nabla \mathbf{N} dv & \int_v \nabla^T \mathbf{W}_u \mathbf{D}\varepsilon_o b_d v_d \mathbf{N} dv \\ \int_v (\nabla^T \mathbf{W}_\rho \frac{b_d}{|b_d|})\rho_d \lambda_d \varepsilon_o \mathbf{D}\nabla \mathbf{N} dv & \int_v (\nabla^T \mathbf{W}_\rho \frac{b_d}{|b_d|}) v_d \mathbf{N} dv \end{array} \right] \tag{28}$$

In the present formulation the Galerkin method has been applied, i.e. $\mathbf{W}_\rho = \mathbf{W}_u = \mathbf{N}$.

### Numerical example

Let us consider the possibilities concerning the boundary conditions to the set of equations (13)-(15) corresponding, respectively, to the variables $\mathbf{u}$, $\rho_d$ and $\gamma_p$. For the first we can specify either displacements or boundary tensions, while for the second, dislocation density values or dislocation flux $q = \mathbf{n} \cdot \mathbf{v}_d \rho_d$. However we can notice that equation (15) does not require boundary conditions. In our simulation a square region of 108nm × 108nm, has been divided into 402 elements as shown in fig.1a, with a refinement up to an element size of 1nm in the region where the dislocation field is expected to propagate (fig 1b). The domain has been fixed by constraining the vertical displacements in the lower boundary and by additionally fixing the horizontal displacement of the left lower corner node, in order to eliminate rigid body motion. On the left boundary nodal forces are imposed which induce a shear stress field $\sigma_{xy}$, see fig.2. The material constants used in this simulation are summarized in table 1. With respect to the initial conditions for the dislocation density field, it is worth to point out that the developed numerical algorithm does not allow to directly specify an initial field for it with automatic generation of the corresponding (according to equation (16)) residual stress

| | Physical quantity | Value |
|---|---|---|
| Kirchhoff modulus | G | $0.3 \times 10^5$ MPa |
| Young modulus | E | $0.7 \times 10^5$ MPa |
| Burgers' vector | b | 0.3 nm |
| Viscosity coefficient | $\lambda_d$ | $1 \times 10^{-6} \frac{m}{s \cdot MPa}$ |

Table 1: Material constants used in the model

field. For this reason, zero initial dislocation density has been assumed in all the discretized domain, $\rho_d(x,t)|_{t=0} \equiv 0$, so that $\gamma_p(x,t)|_{t=0} \equiv 0$, and additionally, a constant-in-time incoming dislocation flux $q = 1 \times 10^{-11} m^{-1} s^{-1}$ is specified between nodes 85 and 105. For the rest of the boundary $\rho_d = 0$ is imposed. Edge dislocations are being modelled, and the Burgers' vector components are

$$b_x = \cos 20° \cdot 0.3 \text{nm} \tag{29}$$

$$b_y = \sin 20° \cdot 0.3 \text{nm} \tag{30}$$

The dislocation entering into the discretized domain propagate across the elements dragged by the forces arising from the stress field. Under the effect of the flowing dislocation field the discretized domain becomes gradually unloaded. Figure 3 shows the stress field at the end of the process, while figure 6 presents the final configuration after 25 times magnification of the displacement field.

### Conclusions from the computer simulation

The formulation presented here is one of the first attempts of simultaneous application of the continuum theory of discolations and the finite element method for computer simulation of elastic–plastic deformation processes. In what concerns the deformation mechanism description (plastic flow rule), the continuum dislocation theory results directly from the mathematical description of experimental observations. On the other hand from the qualitative analysis of the obtained results, it should be said that they remind rather a heat diffusion process in a continuous medium than the really observed dislocation motion. We can ask *Which is the main reason for the qualitative differences between the real dislocation flow process and the computer simulation results?* In the authors' opinion, it is not due to an erroneous kinematic assumption in the continuum theory of dislocations (plastic flow rule), because the process history does not depend only on the kinematic assumptions, but and mostly, on the thermodynamic forces which govern the process. To appreciate what an essential role these forces have in the qualitative evolution of the plastic deformation process, it suffices to compare photographs of the deformed microstructure pattern corresponding to materials with low and high stacking fault energy.

A crucial question arises, then: which forces should be considered in the continuum theory of dislocations, in order to have a better description of the problem. An important argument here is that material structures corresponding to a quasi-uniform field of monomial dislocations are not found in practice. Moreover, in spite of the fact that the dislocation motion is generally accepted as the fundamental mechanism of crystal plastic deformation, the lattice curvature observed in monocrystals are usually measured not in degrees but in minutes. This fact supports the statement that structures with high dislocation density tensor (that is, high lattice distortion) are a very high energy structures. Therefore, when in the continuum theory of dislocations the dislocation field $\alpha_d(x,t)$ is assumed, it should not be simultaneously assumed also that the free energy does not depend on $\alpha_d$. Unfortunately to such assumption, which is classical in the continuum theory, we have limited in numerical implementations.

$\sigma_{\mathbf{xx}})$
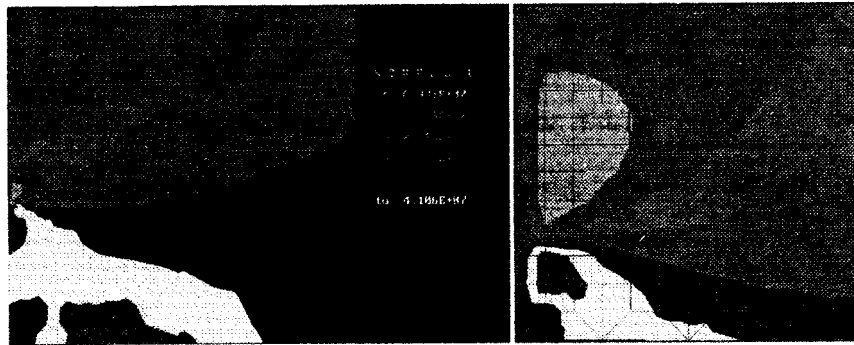


$\sigma_{\mathbf{xy}})$
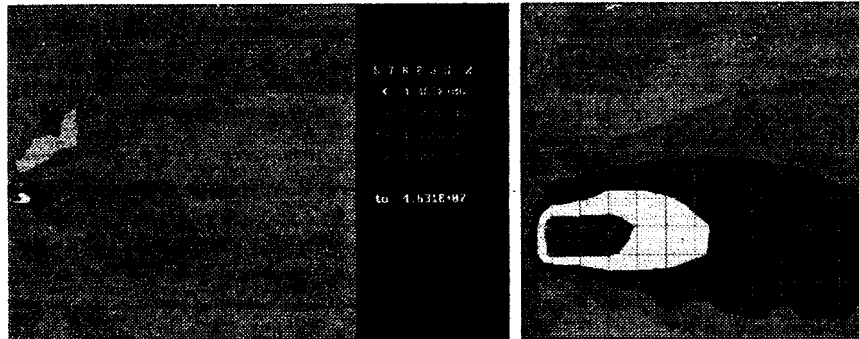


$\sigma_{\mathbf{yy}})$
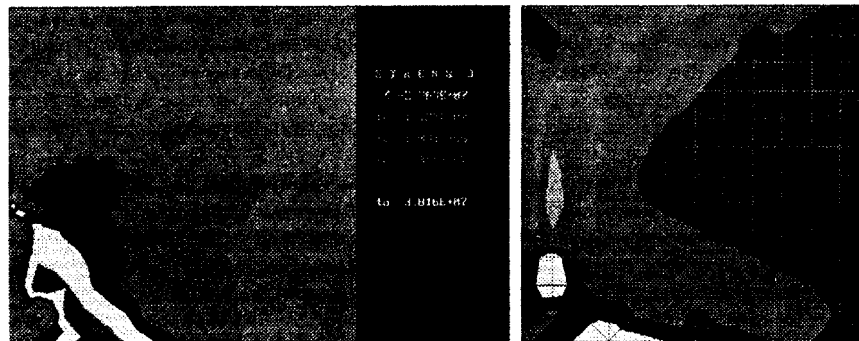


Figure 2: State of stress in [MPa], at time $t = 0$, — right: detailed view of the area with highest stress gradient

$\sigma_{xx}$)
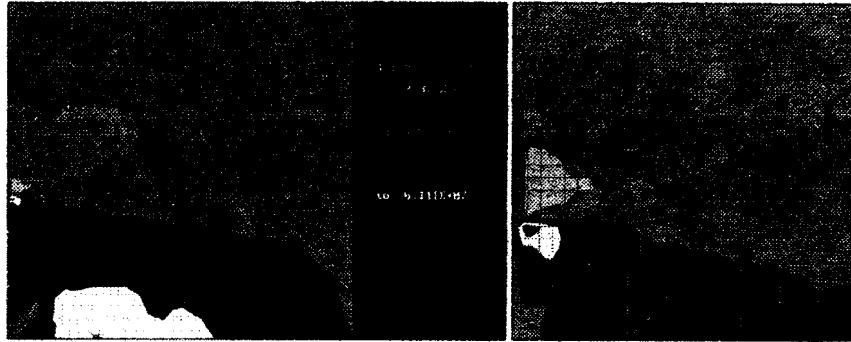


$\sigma_{xy}$)
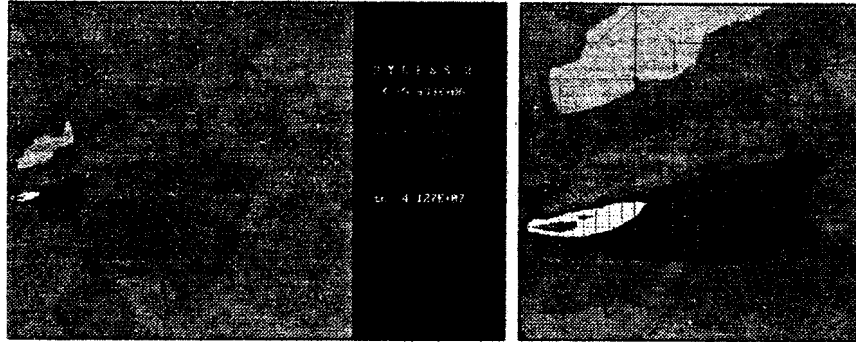


$\sigma_{yy}$)
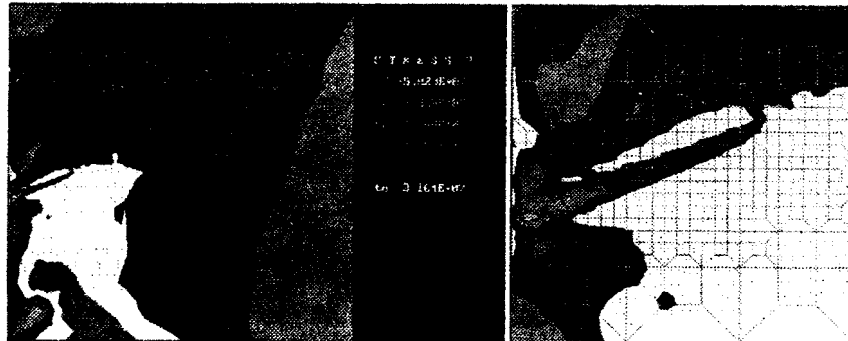


Figure 3: Final state of stress (obtained for $t = 1.2s$)

t = 0.2s)
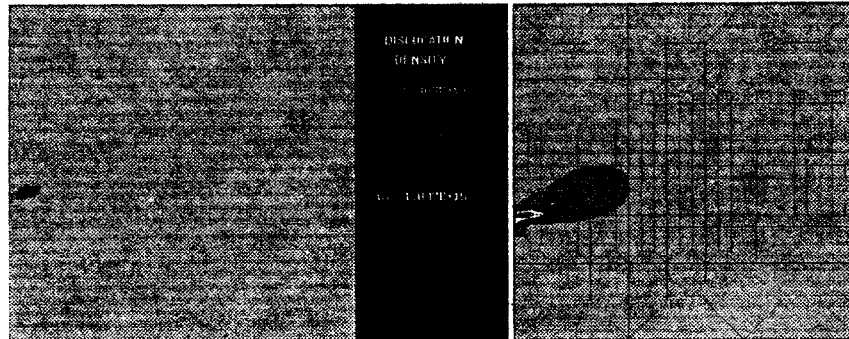


t = 0.4s)
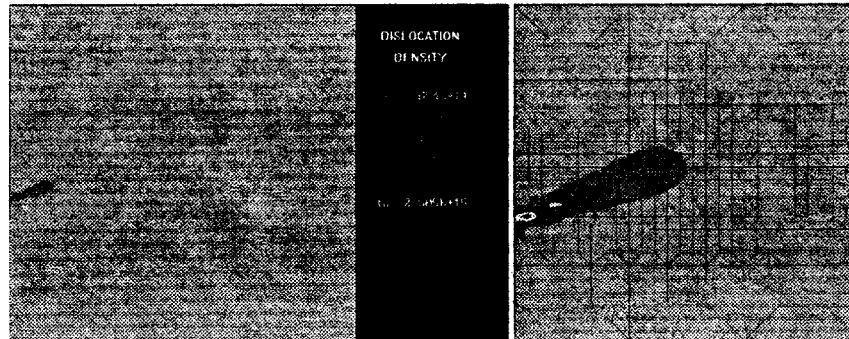


t = 0.6s)
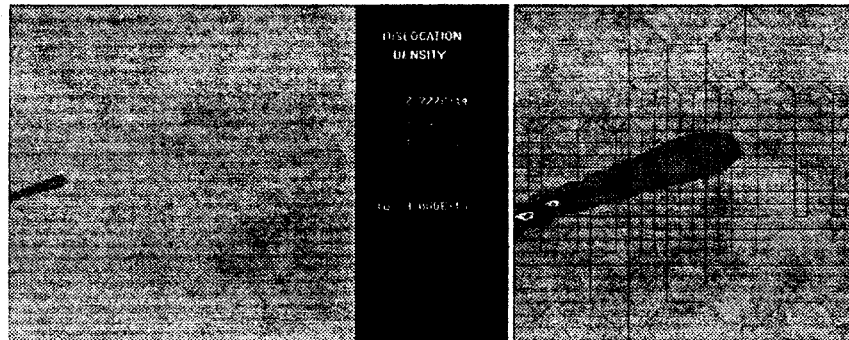


Figure 4: Sequential stages of dislocation density field propagation, continued in the next figure

t = 0.8s)
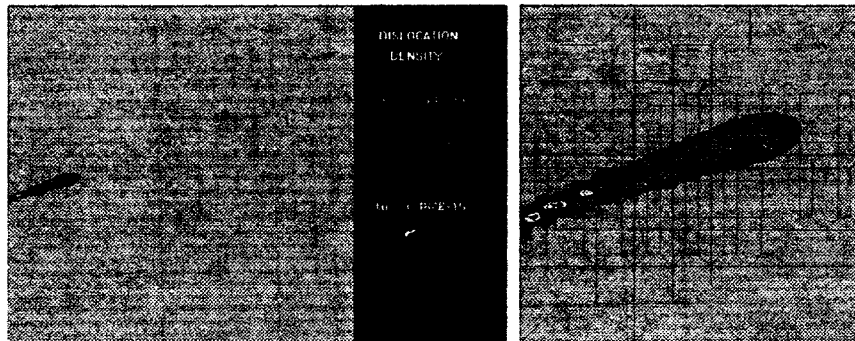


t = 1.0s)
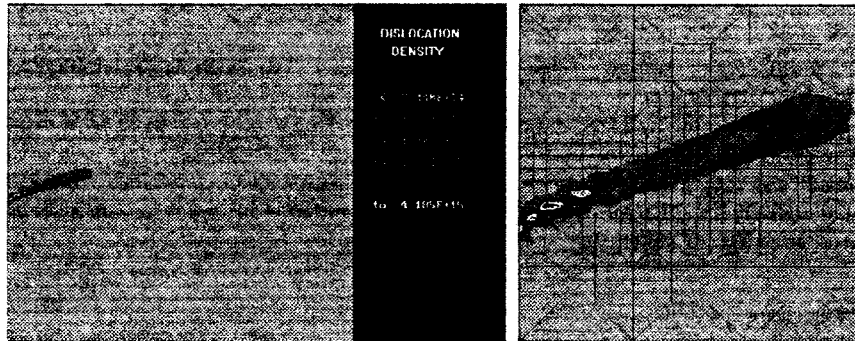


t = 1.2s)
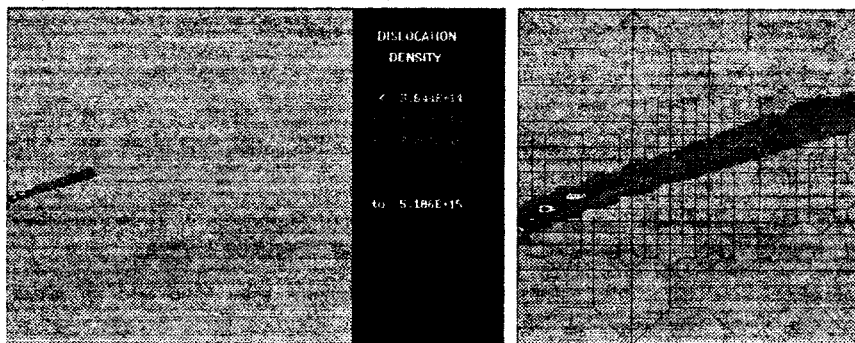


Figure 5: Sequential stages of dislocation density field propagation
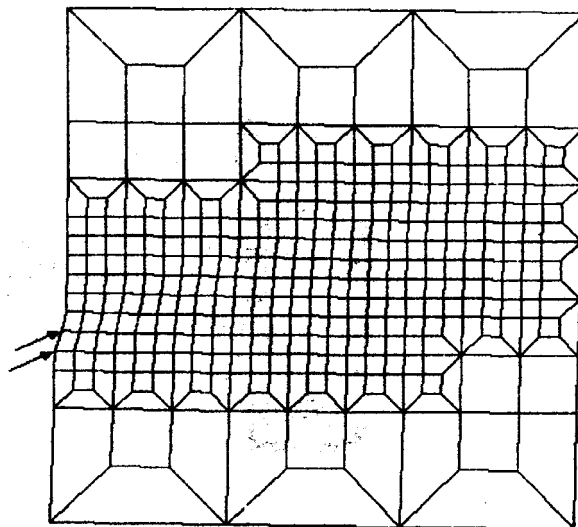
Figure 6: A fragment of the final configuration (t=1.2s) with a 25 times displacement magnification.

# References

[1] Canova G.R., Bréchet Y., Kubin L.P., Devincre B., Pontikis V. & Condat M., 3D simulation of dislocation motion on a lattice. Proc. Int. Coll. DISLOCATIONS 93 -Microstructures and Physical Properties (ed. L.P.Kubin et al.) Aussois 31 March-9 April, (1993) France.

[2] Dłużewski P. On geometry and continuum thermodynamics of structural defect movement. *Mech. Mater.* **22**, 23-41 (1996).

[3] Dłużewski P. & Antúnez H. Finite element simulation of dislocation field movement. *CAMES* 2, 141-148 (1995).

[4] Mura T., Method of continuously distributed dislocations. *Mathematical Theory of Dislocations* (ed. T. Mura), 25-48. The American Soc. Mech. Engineers, New York (1969).

[5] Peach M.O., & Koehler J.S., (1950) The forces exerted on dislocations and the stress fields produced by them. *Phys. Rev.* **80**, 436.

[6] Stigh U., (1993) A finite element study of treading dislocations. *Mech. Mater.* **14**, 179 187.

[7] Zienkiewicz O.C. & Taylor R.J., *The Finite Element Method* 4th ed. Vol.2, McGraw-Hill, London (1991).